

# Exact quantum dynamics of a bosonic Josephson junction

Kaspar Sakmann, Alexej I. Streltsov, Ofir E. Alon and Lorenz S. Cederbaum  
*Theoretische Chemie, Physikalisch-Chemisches Institut, Universität Heidelberg,  
Im Neuenheimer Feld 229, D-69120 Heidelberg, Germany*

## Abstract

The quantum dynamics of a one-dimensional bosonic Josephson junction is studied by solving the time-dependent many-boson Schrödinger equation numerically exactly. Already for weak interparticle interactions and on short time scales, the commonly-employed mean-field and many-body methods are found to deviate substantially from the exact dynamics. The system exhibits rich many-body dynamics like enhanced tunneling and a novel equilibration phenomenon of the junction depending on the interaction, attributed to a quick loss of coherence.

PACS numbers: 03.75.Kk, 03.75.Lm, 05.30.Jp, 03.65.-w

Recent experiments on interacting Bose-Einstein condensates in double-well traps have led to some of the most exciting results in quantum physics, including matter-wave interferometry [1, 2], squeezing and entanglement [3, 4] as well as work on high-precision sensors [5]. Particular attention has been paid to tunneling phenomena of interacting Bose-Einstein condensates in double-wells, which in this context are referred to as bosonic Josephson junctions. Explicitly, Josephson oscillations and self-trapping (suppression of tunneling) with Bose-Einstein condensates have been predicted [6, 7] and recently realized in experiments [8, 9], drawing intensive interest, see, e.g., [10, 11, 12, 13, 14, 15] and references therein.

For the first time in literature we provide the numerically exact many-body quantum dynamics of a one-dimensional (1D) bosonic Josephson junction in this work. This is made possible by a breakthrough in the solution of the time-dependent many-boson Schrödinger equation. We use the exact solution to check the current understanding of bosonic Josephson junctions – commonly described by the popular Gross-Pitaevskii (GP) mean-field theory and the Bose-Hubbard (BH) many-body model – and to find novel phenomena. The results of the GP and BH theories are found to deviate substantially from the full many-body solution, already for weak interactions and on short time scales. In particular, the well-known self-trapping effect is greatly reduced. We attribute these findings to a quick loss of the junction’s coherence not captured by the common methods. For stronger interactions and on longer time scales, we find a novel equilibration dynamics in which the density and other observables of the junction tend towards stationary values. We show that the dynamics of bosonic Josephson junctions is much richer than what is currently known.

To compute the time evolution of the system, we solve the time-dependent many-boson Schrödinger equation by using the multiconfigurational time-dependent Hartree for bosons (MCTDHB) method [16]. In the MCTDHB( $M$ ) method the time-dependent many-boson wavefunction is expanded in all time-dependent permanents  $|\vec{n}; t\rangle$ , generated by distributing  $N$  bosons over  $M$  time-dependent orbitals  $\{\phi_i(x, t)\}$ .  $\vec{n} = (n_1, n_2, \dots, n_M)$  collects the occupation numbers. The MCTDHB wavefunction thus reads  $|\Psi(t)\rangle = \sum_{\vec{n}} C_{\vec{n}}(t) |\vec{n}; t\rangle$ . The expansion coefficients  $\{C_{\vec{n}}(t)\}$  and the orbitals  $\{\phi_i(x, t)\}$  are determined by the Dirac-Frenkel time-dependent variational principle [16]. The present results are obtained by using a novel mapping of the many-boson configuration space in combination with a parallel implementation of MCTDHB, allowing the efficient handling of millions of time-dependent, optimized permanents [17]. We note that GP theory is contained in the MCTDHB framework as the

special case  $M = 1$ . The many-body wavefunction then becomes a single permanent and the dynamics is restricted to remaining condensed at all times. The BH model for this system employs two orbitals and is thus, in principle, capable of describing correlations. However, as we shall see below, the fact that the BH orbitals are *time-independent* causes the BH model to underestimate correlations.

With the time-dependent many-boson wavefunction  $|\Psi(t)\rangle$  at hand, any quantity of interest of the interacting many-boson system can be computed. Here we focus on the evolution of the following quantities to analyze the dynamics of the Josephson junction. The reduced one-body density matrix of the system is defined by  $\rho^{(1)}(x|x';t) = \langle \Psi(t) | \hat{\Psi}^\dagger(x') \hat{\Psi}(x) | \Psi(t) \rangle$ , where  $\hat{\Psi}(x)$  is the usual bosonic field operator annihilating a particle at position  $x$ . Its diagonal part,  $\rho(x,t) \equiv \rho^{(1)}(x|x' = x;t)$ , is simply the density of the system. As is common in the analysis of bosonic Josephson junctions, the “survival probability” of the system in, e.g., the left well, is obtained by integrating the density over the left well,  $p_L(t) \equiv \frac{1}{N} \int_{-\infty}^0 \rho(x,t) dx$ . Furthermore, the eigenvalues  $n_i^{(1)}$  of  $\rho^{(1)}(x|x';t)$  determine the extent to which the system is condensed or fragmented [18, 19]. Finally, the first-order correlation function  $g^{(1)}(x',x;t) \equiv \rho^{(1)}(x|x';t) / \sqrt{\rho(x,t)\rho(x',t)}$  quantifies the system’s degree of spatial coherence [20, 21].

We now turn to the details of the 1D bosonic Josephson junction considered in this work. It is convenient to use dimensionless units defined by dividing the Hamiltonian by  $\frac{\hbar^2}{mL^2}$ , where  $m$  is the mass of a boson, e.g.,  $^{87}\text{Rb}$  and  $L$  is a length scale, e.g.,  $L = 1\mu m$ . One unit of energy then corresponds to 116 Hz. We have a 1D realization of an experimental setup similar to the one in Ref. [8] in mind. The full many-body Hamiltonian then reads  $H = \sum_{i=1}^N h(x_i) + \sum_{i<j} W(x_i - x_j)$ , where  $h(x) = -\frac{1}{2} \frac{\partial^2}{\partial x^2} + V(x)$ , with a trapping potential  $V(x)$  and an interparticle interaction potential  $W(x - x') = \lambda_0 \delta(x - x')$ .

The double-well potential  $V(x)$  is generated by connecting two harmonic potentials  $V_{\pm}(x) = \frac{1}{2}(x \pm 2)^2$  with a cubic spline in the region  $|x| \leq 0.5$ . This results in a symmetric double-well potential with barrier height  $V(0) = 1.667$ . The lowest four single-particle energy levels  $e_1 = 0.473, e_2 = 0.518, e_3 = 1.352$  and  $e_4 = 1.611$  of  $V(x)$  are lower than the barrier.

Left- and right-localized orbitals  $\phi_{L,R}$  can be constructed from the single-particle ground state and the first excited state of  $V(x)$ .  $\phi_L$  and  $\phi_R$  determine the parameters  $U = \lambda_0 \int |\phi_L|^4$ ,  $J = -\int \phi_L^* h \phi_R$ , the Rabi oscillation period  $t_{Rabi} = \pi/J$  and the often employed interaction

parameters,  $\Lambda = UN/(2J)$  and  $U/J$  [6, 7]. In this work we use the interaction parameter  $\lambda = \lambda_0(N - 1)$ , which appears naturally in the full many-body treatment, and quote the corresponding values for  $\Lambda$  and  $U/J$ . Within the framework of two-mode GP theory, a state, which is initially localized in one well, is predicted to remain *self-trapped* if  $\Lambda > \Lambda_c = 2$  [6, 7]. We will consider interaction strengths below, in the vicinity of and above  $\Lambda_c$ .

In all our computations the system is prepared at  $t = 0$  as the many-body ground state of the potential  $V_+(x)$  and then propagated in the potential  $V(x)$ . Within the BH framework this procedure amounts to starting from the state in which all bosons occupy the orbital  $\phi_L$ .

We begin our studies with a weak interaction strength  $\lambda = 0.152$ , leading to  $U/J = 0.140$  (0.027) and  $\Lambda = 1.40$  (1.35) for  $N = 20$  (100) bosons, which is well below the transition point for self-trapping  $\Lambda_c = 2$ . In the upper two panels of Fig. 1 the full many-body (solid blue lines) results for  $p_L(t)$  are shown together with those of GP (solid black lines) and BH (solid magenta lines) theory. The full many-body dynamics is governed by three different time scales. On a time scale of the order of a Rabi cycle,  $p_L(t)$  performs large-amplitude oscillations about  $p_L = 0.5$ , the long time average of  $p_L(t)$ . The amplitude of these oscillations is damped out on a time scale of a few Rabi cycles and marks the beginning of a collapse and revival (not shown) sequence [6], confirmed here on the full many-body level. On top of these slow large-amplitude oscillations, a higher frequency with a small amplitude can be seen. In a single-particle picture these high frequency oscillations can be related to contributions from higher excited states in the initial wavefunction. However, a single particle picture fails to describe the dynamics, as we shall now show. While the initial wavefunction  $|\Psi(t = 0)\rangle$  is practically condensed – the fragmentation of the system is less than  $10^{-4}$  ( $10^{-5}$ ) for  $N = 20$  (100) bosons – the propagated wavefunction  $|\Psi(t)\rangle$  quickly becomes fragmented. The fragmentation increases to about 33% (26%) at  $t = 3t_{Rabi}$  for  $N = 20$  (100) particles, making a many-body treatment indispensable, already at this weak interaction strength. The respective GP results (solid black lines) oscillate back and forth at a frequency close to the Rabi frequency and resemble the full many-body dynamics only on a time scale *shorter* than half a Rabi cycle. The poor quality of the GP mean-field approximation is, of course, due to the fact that the exact wavefunction starts to fragment while the GP dynamics remains condensed by construction.

The BH (solid magenta line) result for  $p_L(t)$  reproduces many features of that of the full many-body solution at this interaction strength for both  $N = 20$  and  $N = 100$  particles.

The large-amplitude oscillations collapse over a period of a few Rabi cycles and revive at a later stage (not shown). Also the BH solution quickly becomes fragmented, starting from the left localized state, which is totally condensed. The fragmentation of the BH wavefunction for  $N = 20$  (100) particles at  $t = 3t_{Rabi}$  is essentially the same as the respective value of the exact solution. However, differences between the exact and the BH result are visible even on time scales less than half a Rabi cycle. Not only are the amplitudes obviously different, but also the frequencies contained in  $p_L(t)$ . Furthermore, the BH solutions do not exhibit a high frequency oscillation on top of the slow large-amplitude oscillations; a difference which is related to the fact that the BH orbitals are *time-independent* and thus, not determined variationally at each point in time. Note that  $p_L(t)$  is a quantity in which *all* spatial degrees of freedom have been integrated out. Visible differences in  $p_L(t)$  imply that it is not only the densities  $\rho(x, t)$  which must differ, but also *all* correlation functions.

The insets of Fig. 1(a),(b) demonstrate the convergence of the many-body dynamics results. In particular and somewhat unexpectedly, the number of *time-dependent* orbitals needed to describe the bosonic Josephson junction dynamics quantitatively is  $M = 4$ , even below the transition point for self-trapping. These orbitals are determined variationally *at each point in time*, implying that any method using time-independent orbitals will need substantially more orbitals to achieve the same accuracy.

One of the central phenomena often discussed in the context of bosonic Josephson junctions is the celebrated transition to self-trapping [6, 7, 8, 9]. In what follows we would like to study the dynamics of a bosonic Josephson junction in the self-trapping regime from the full many-body perspective.

The interaction strength is taken to be  $\lambda = 0.245$ , leading to  $U/J = 0.226$  (0.043) and  $\Lambda = 2.26$  (2.17) for  $N = 20$  (100) particles. Hence, the system is just above the critical value for self-trapping  $\Lambda_c = 2$  [6, 7]. The results for  $N = 20$  and  $N = 100$  are collected in Fig. 1(c),(d). We find that the full many-body solutions (solid blue lines) exhibit indeed some self-trapping on the time scale shown. The fragmentation of the condensate for  $N = 20$  (100) bosons increases from initially less than  $10^{-4}$  ( $10^{-5}$ ) to about 28% (18%) after three Rabi cycles. Note that the system is now *less* fragmented than for weaker interactions after the same period of time. Nevertheless, GP (solid black lines) theory is – as before – inapplicable, even on time scales shorter than  $t_{Rabi}/2$ . The BH (solid magenta lines) results deviate from the true dynamics even earlier. They greatly overestimate the self-trapping

and coherence of the condensate. According to the BH model the condensate would only be 13% (11%) fragmented for  $N = 20$  (100) at  $t = 3t_{Rabi}$ , which is not the case. This trend also continues for stronger interactions, see below. The following general statement about the relationship between self-trapping and coherence can be inferred from our full many-body results: Self-trapping is *only* present as long as the system remains coherent. We find this statement to be true at all interaction strengths and all particle numbers considered in this work.

We now turn to the case of stronger interactions,  $\lambda = 4.9$ , which is well above the self-trapping transition point. This leads to  $U/J = 9.55$  (0.869) and  $\Lambda = 47.8$  (43.4) for  $N = 10$  (100) bosons. Note that we now use ten instead of twenty bosons to demonstrate convergence. The energy per particle of the full many-body wavefunction is now  $E/N = 1.22$  (1.28) for  $N = 10$  (100) bosons, which is still below the barrier height  $V(0) = 1.667$ . What do we expect to happen? According to two-mode GP theory, the density should remain trapped in the initial well for any interaction strength  $\Lambda \gg \Lambda_c$  [6, 7]. Similarly, the BH model predicts ever increasing tunneling times since the left- and right-localized states become eigenstates of the BH Hamiltonian in the limit  $U/J \rightarrow \infty$  [6]. These predictions are incorrect for stronger interactions since the repulsive interaction leads to fragmentation and broadening of the initial wavefunction, thereby facilitating tunneling. The impact of the potential barrier therefore decreases with increasing interaction strength. We will now show that a very intricate dynamics results.

Fig. 2(top) shows the full many-body results for  $N = 10$  (solid blue line) and  $N = 100$  (solid green line) bosons together with those of the BH (solid magenta line) model. The two BH results lie on top of each other. In complete contrast to the BH dynamics, for which  $p_L(t)$  remains trapped in the left well, the full many-body dynamics shows no self-trapping. Instead, an equilibration phenomenon emerges, in which the density of the system tends to be equally distributed over both wells.

The system's full many-body dynamics is again strongly fragmented as can be seen in Fig. 2(bottom), which depicts the natural-orbital occupations  $n_i^{(1)}$  (solid blue lines) for  $N = 10$  particles. This rules out any description of the system by GP mean-field theory. Also shown are the natural-orbital occupations of the BH (solid magenta lines) model, which wrongly describes a fully condensed system.

The strong fragmentation of the system implies the presence of strong correlations. This

can be seen in the two upper panels of Fig. 3, which show the full many-body result for the first-order correlation function  $g^{(1)}(x', x; t)$  of  $N = 10$  bosons at times  $t = 0$  (top left) and  $t = 10t_{Rabi}$  (top right). The fragmentation of the initial state is only  $\approx 2\%$ , leading to an almost flat  $g^{(1)}(x', x; 0)$ . This reflects the fact that the system is initially coherent over its entire extent. At  $t = 10t_{Rabi}$  the coherence of the system is completely lost even on length scales much shorter than its size, see upper right panel of Fig. 3. Note that also  $g^{(1)}(x', x; t)$  tends to equilibrate. The respective BH results for  $g^{(1)}(x', x; t)$  are shown in the two lower panels of Fig. 3 and in contrast display no visible loss of coherence.

Let us briefly summarize. We have obtained exact results for the full many-body dynamics of 1D bosonic Josephson junctions. The dynamics is found to be much richer than previously reported. In particular, the predictions of the commonly-employed Gross-Pitaevskii and Bose-Hubbard theories are found to differ substantially from the exact results, already after short times and relatively weak interactions. These differences are associated with the development of fragmentation and correlations not captured by the standard theories. For stronger interactions, where the standard theories predict coherence and self-trapping, we find a completely different dynamics. The system becomes fragmented, spatial coherence is lost and a long-time equilibration of the junction emerges. We hope our results stimulate experiments.

Financial support by the DFG is acknowledged.

- 
- [1] M. R. Andrews *et al.*, Science **275**, 637 (1997).
  - [2] T. Schumm *et al.*, Nature Physics **1**, 57 (2005).
  - [3] G.-B. Jo *et al.*, Phys. Rev. Lett. **98**, 030407 (2007).
  - [4] J. Estève *et al.*, Nature **455**, 1216 (2008).
  - [5] B. V. Hall *et al.*, Phys. Rev. Lett. **98**, 030402 (2007).
  - [6] G. J. Milburn *et al.*, Phys. Rev. A **55**, 4318 (1997).
  - [7] A. Smerzi *et al.*, Phys. Rev. Lett. **79**, 4950 (1997).
  - [8] M. Albiez *et al.*, Phys. Rev. Lett. **95**, 010402 (2005).
  - [9] S. Levy *et al.*, Nature, **449**, 579 (2007).
  - [10] S. Raghavan *et al.*, Phys. Rev. A **59**, 620 (1999).

- [11] C. Lee, Phys. Rev. Lett. **97**, 150402 (2006).
- [12] D. Ananikian and T. Bergeman, Phys. Rev. A **73**, 013604 (2006).
- [13] R. Gati and M. K. Oberthaler, J. Phys. B **40**, R61 (2007).
- [14] G. Ferrini *et al.*, Phys. Rev. A **78**, 023606 (2008).
- [15] X. Y. Jia *et al.*, Phys. Rev. A **78**, 023613 (2008).
- [16] A. I. Streltsov *et al.*, Phys. Rev. Lett. **99**, 030402 (2007); O. E. Alon *et al.*, Phys. Rev. A **77**, 033613 (2008).
- [17] A. I. Streltsov *et al.* (to be submitted).
- [18] A. I. Streltsov *et al.*, Phys. Rev. A **73**, 063626 (2006).
- [19] E. J. Mueller *et al.*, Phys. Rev. A **74**, 033612 (2006).
- [20] M. Naraschewski and R. J. Glauber, Phys. Rev. A **59**, 4595 (1999).
- [21] K. Sakmann *et al.*, Phys. Rev. A **78**, 023615 (2008).



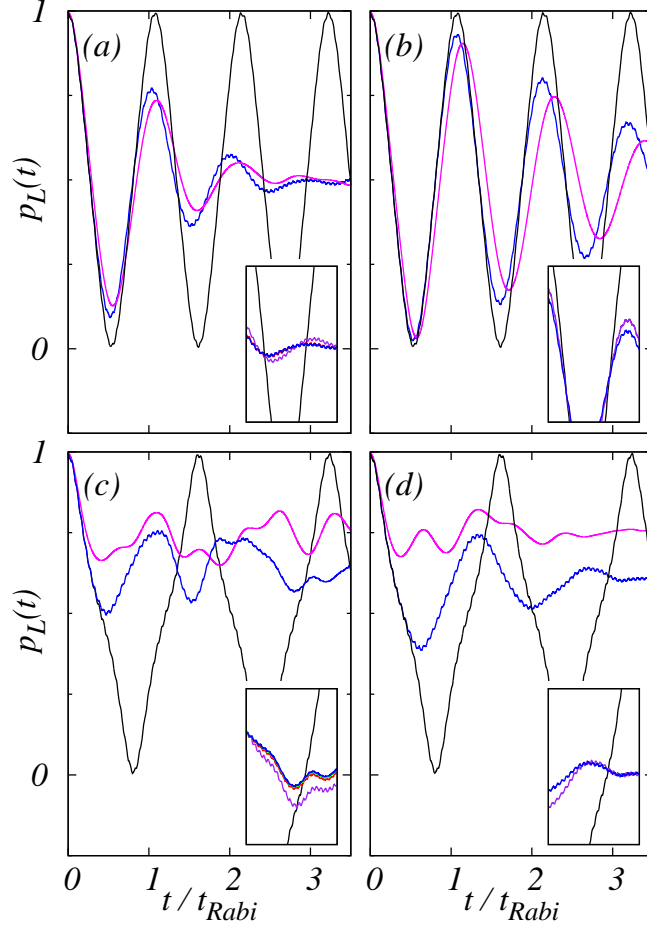


FIG. 1: (Color online) Full quantum dynamics of a 1D bosonic Josephson junction below and above the transition to self-trapping. Shown is the full many-body result (solid blue lines) for the probability of finding a boson in the left well,  $p_L(t)$ . For comparison, the respective GP (solid black lines) and BH (solid magenta lines) results are shown as well. The parameter values are: (a)  $N = 20$ ,  $\lambda = 0.152$  and (b)  $N = 100$ ,  $\lambda = 0.152$  (below the self-trapping transition), (c)  $N = 20$ ,  $\lambda = 0.245$  and (d)  $N = 100$ ,  $\lambda = 0.245$  (above the self-trapping transition). The GP and BH results are found to deviate from the full many-body results already after short times. The insets show the convergence of the full many-body results. (a),(c):  $M = 2$  (solid purple line),  $M = 4$  (solid red line),  $M = 6$  (solid green line),  $M = 8$  (solid blue line). The  $M = 2$  results are seen to deviate slightly from the converged results for  $M \geq 4$ . (b),(d): The results for  $M = 2$  (solid purple line) and  $M = 4$  (solid blue line) are shown. All quantities shown are dimensionless.

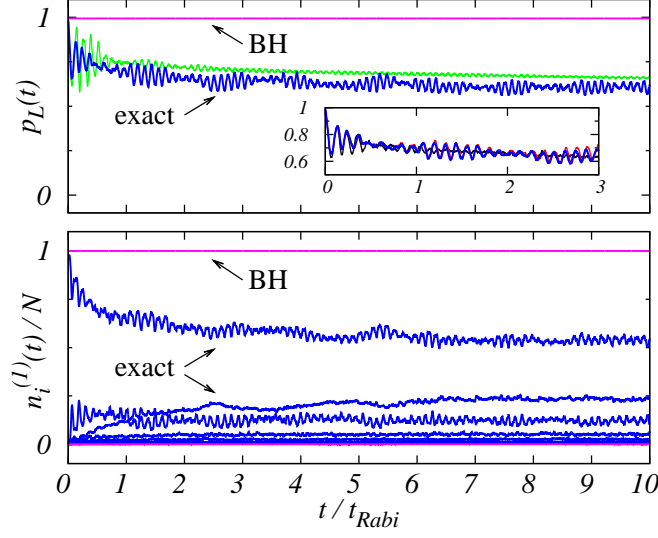


FIG. 2: (Color online) Emergence of equilibration of the density at interaction strength  $\lambda = 4.9$ . Top: same as Fig. 1, but for  $N = 10$  (solid blue line) and  $N = 100$  (solid green line). The respective BH (solid magenta lines) results are on top of each other. In contrast to the BH dynamics which is completely self-trapped, the full many-body dynamics is not.  $p_L(t)$  tends towards its long-time average  $p_L = 0.5$ . For  $N = 100$  particles  $M = 4$  orbitals were used. The inset shows the convergence of the full many-body solution for  $N = 10$  bosons:  $M = 4$  (solid black line),  $M = 10$  (solid blue line),  $M = 12$  (solid red line). The  $M = 4$  result follows the trend of the converged  $M = 12$  result. Bottom: corresponding natural orbital occupations for  $N = 10$  bosons. The system becomes fragmented and roughly four natural orbitals are macroscopically occupied. All quantities are dimensionless.

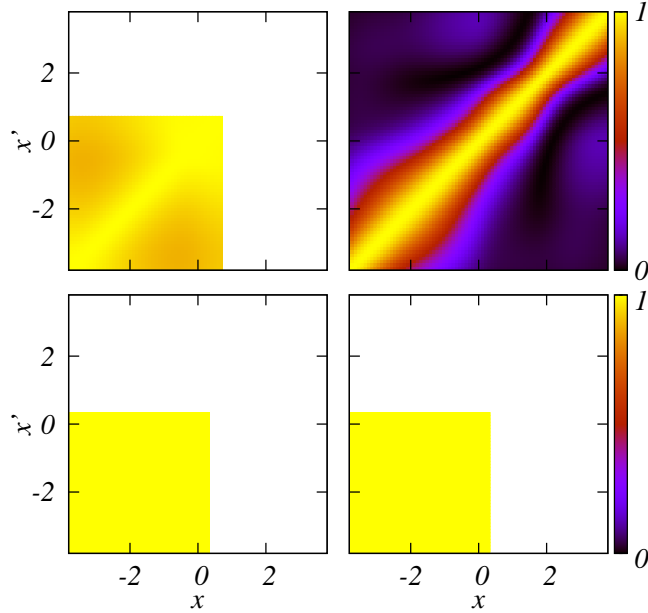


FIG. 3: (Color online) Dynamics of the first order correlation function for  $\lambda = 4.9$  at which the equilibration phenomenon of Fig. 2 occurs. Shown is  $|g^{(1)}(x', x; t)|^2$  of  $N = 10$  bosons at different times. Top left: full many-body result at  $t = 0$ . The initial state exhibits coherence over the entire extent of the system. Top right: full many-body result at  $t = 10t_{Rabi}$ . The coherence is lost. The system is incoherent even on short length scales. Bottom left: BH result at  $t = 0$ . Bottom right: BH result at  $t = 10t_{Rabi}$ . In contrast to the full many-body result, the BH wavefunction remains completely coherent.